High quality *Y*-type hexaferrite thick films for microwave applications by an economical and environmentally benign crystal growth technique

Bolin Hu,[1] Yajie Chen,[1,a)] Scott Gillette,[1] Zhijuan Su,[1] Jason Wolf,[2] Michael E. McHenry,[2] and Vincent G. Harris[1]
[1]*Center for Microwave Magnetic Materials and Integrated Circuits and Department of Electrical and Computer Engineering, Northeastern University, Boston, Massachusetts 02115, USA*
[2]*Materials Science and Engineering, Carnegie Mellon University, Pittsburgh, Pennsylvania 15213, USA*

(Received 12 November 2013; accepted 4 February 2014; published online 20 February 2014)

Thick barium hexaferrite $Ba_2Zn_2Fe_{12}O_{22}$ (i.e., Zn_2Y) films having thicknesses of $\sim$100 μm were epitaxially grown on MgO (111) substrates using an environmentally benign ferrite-salt mixture by vaporizing the salt. X-ray diffraction pole figure analyses showed (00*l*) crystallographic alignment with little in plane dispersion confirming epitaxial growth. Saturation magnetization, $4\pi M_s$, was measured for as-grown films to be 2.51 ± 0.1 kG with an out of plane magnetic anisotropy field H_A of 8.9 ± 0.1 kOe. Ferromagnetic resonance linewidth, as the peak-to-peak power absorption derivative at 9.6 GHz, was measured to be 62 Oe. These properties demonstrate a rapid, convenient, cost-effective, and nontoxic method of growing high quality thick crystalline ferrite films which could be used widely for microwave device applications. © *2014 AIP Publishing LLC*. [http://dx.doi.org/10.1063/1.4866026]

The present microwave integrated circuit design paradigm has passive circuit elements, e.g., ferrite-based isolators, circulators, phase shifters, etc., fabricated on dielectric substrates.[1–3] A long sought goal of the microwave device community has been the fabrication of reduced size, weight, and costs of ferrite components while concomitantly enhancing performance and functionality.[1,2] Single crystal or quasi-single crystal ferrites have advantages such as high crystalline orientation, low microwave loss and compact size, and high efficiency in device applications.[4–6] Earlier steps, such as traditional Pt crucible-based crystal flux growth,[7,8] liquid phase epitaxy,[9,10] screen printing,[11] solid-state quasi-crystal growth,[12] and floating zone techniques,[13] were employed to grow low microwave loss ferrite materials. However, those methods require long firing and/or cooling cycles, often complicated laboratory instrumentation and protocols, and expensive chemical materials consumption and waste. Furthermore, traditional growth methods typically involve complicated liquid phase mixtures, strict temperature and growth diffusion rate control, and the use of highly toxic fluxes of the Bi_2O_3 and/or PbO type (among others). These characteristics often result in a higher likelihood of failure, the detrimental introduction of impurities,[14] and environmental pollution. To this end, a technique that realizes epitaxial thick crystalline ferrite film growth on dielectric substrates having a benign environmental impact, low cost, rapid and simple experimental setup, and protocols is sought. Such a technique will have a wide-ranging impact on the field of microwave devices, components, and systems.

Single-crystal Zn_2Y, i.e., $Ba_2Zn_2Fe_{12}O_{22}$, ferrites are an important class of microwave ferrites that are widely considered and used in the design of microwave and mm-wave filters and phase shifters (among other devices). However, it is often difficult to grow Y-type hexaferrites especially with thicknesses in the 10's of microns on lattice matched supporting substrates. In the present work, a method for growing large area, i.e., >1 cm^2, Zn_2Y ferrite crystalline films on single-crystal (111) MgO substrates with thicknesses ranging from 25 to >100 μm is demonstrated. In this technique, a ferrite oxide precursor (FOP) mixture of $BaCO_3$, ZnO, and Fe_2O_3 with mole ratio of 1:1:3 was ball milled for 2 h in alcohol followed by drying at 90 °C in air to eliminate the solvent. The FOP and anhydrous sodium carbonate are then melted on the surface of an MgO single crystal substrate so that the molten solution spreads over the surface as a uniform layer. The solution is maintained at 1050–1150 °C for 5–15 h in order to vaporize the anhydrous sodium carbonate, thus depositing the ferrite film. Ferrite films grow with the same crystallographic orientation as the substrate. The side views of various approaches of applying the FOP and Na_2CO_3 to the substrate are shown in Fig. 1(a). In each experiment, the weight ratio of salt to FOP was maintained at 1:1, and the surface loading of the FOP was 1 mg/mm^2. The magnetic properties of the films were measured using a vibrating sample magnetometer (VSM) at room temperature with a magnetic field strength ranging from -10 kOe to 10 kOe. Both in plane and out of plane hysteresis loops are presented in Fig. 1(b). In method A (see Fig. 1(a) and Table I), a dry mixture of FOP and anhydrous Na_2CO_3 was used, resulting in secondary nucleation and polycrystalline deposits. No obvious magnetic anisotropy was observed in the hysteresis loops of sample A that indicated the sample grew without a preferred crystalline orientation. In method B, an alumina ring was introduced to assist in confining the reactant powders: The salt was packed on the bottom and the FOP loosely placed atop the salt. However, most crystallization took place on the walls of the alumina ring, leaving little ferrite yield on the substrate. Resulting films demonstrated similar in plane and out of plane hysteresis loops with magnetization values lower than published results for Zn_2Y.[14] In method C, dry anhydrous Na_2CO_3 was spread loosely atop

a)Author to whom correspondence should be addressed. Electronic mail: y.chen@neu.edu.

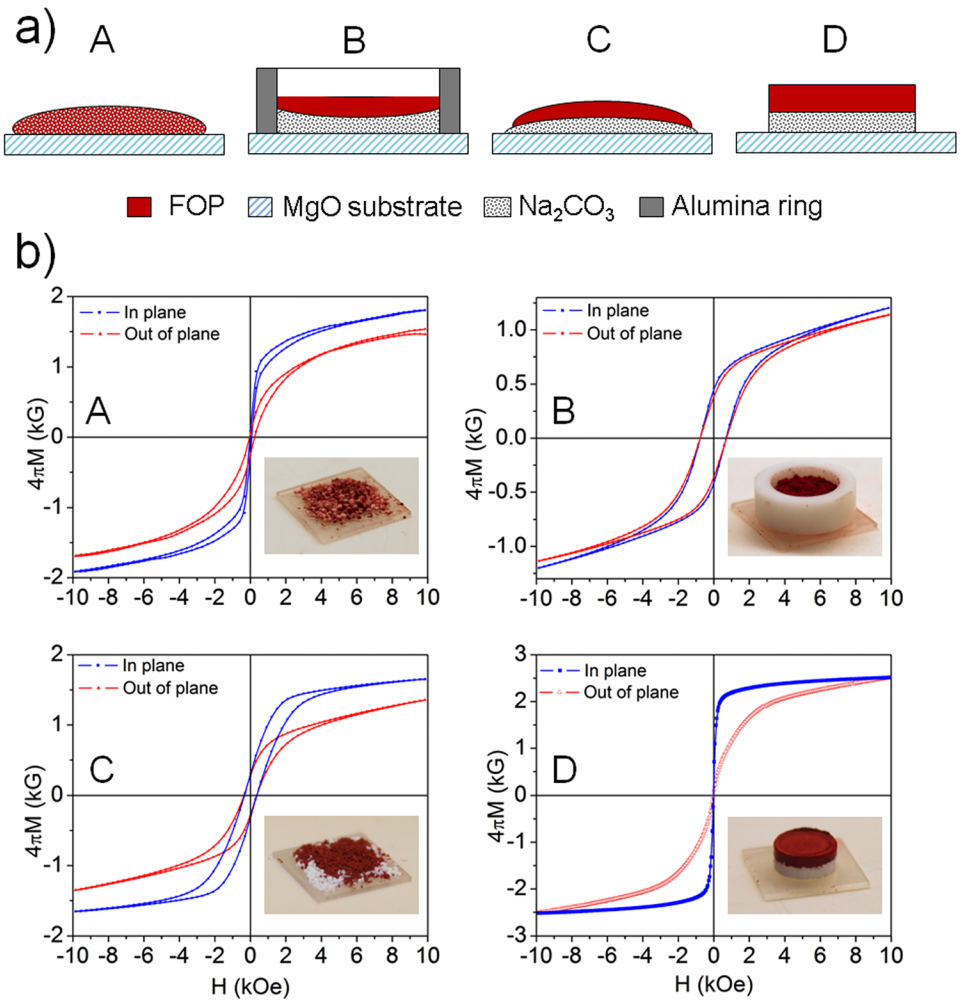

FIG. 1. (a) Images of the experimental set-up for each sample growth approach, and (b) hysteresis loops of Zn_2Y ferrite thick films grown under different conditions with in plane and out of plane applied magnetic field orientation.

the substrate and covered with dry FOP. This approach resulted in relatively poor control of the ferrite concentration as well as an uneven ferrite film thickness. The VSM results indicated a slight in-plane anisotropy and relatively low $4\pi M_s$. Method D, which gave the best results, involved the compaction of a bilayer of dry anhydrous Na_2CO_3 and dry FOP; the disk was then placed on the MgO substrate. VSM results show that the easy axis of the film aligns in the film plane, with a saturation magnetization ($4\pi M_s$) of 2.5 ± 0.1 kG. The out of plane magnetic anisotropy field H_A is of 8.9 ± 0.1 kOe. All values are consistent with those reported in the literature for Zn_2Y.[15]

The ferrite nominal composition and representative firing conditions are listed in Table I. The thickness of the ferrite films was largely dependent upon the thickness of the liquid layer formed on the MgO. The FOP surface loading, temperature, firing time, and weight ratio of salt to FOP, are four key factors affecting the epitaxial growth of ferrite films. In general, the best films, as judged by both crystallinity and magnetic properties, were produced by using the lowest temperature that would facilitate complete melting of the FOP and salt mixture. For the case of the weight ratio of 1:1 between salt and FOP, if the melt had a low viscosity and low surface tension, as is the case for low FOP surface

TABLE I. Ferrite thick film growth conditions.

Variable Exp. condition	FOP weight (%)	FOP surface loading (mg/mm^2)	Time (h)	Temp. (°C)	Film thickness (μm)	Comments
Surface loading	50	1.67	15	1100	N/A	Excess melts run off substrate
	50	1.33	15	1100	~100	Uniform surface
	50	1	15	1100	~80	Uniform surface
Firing time	50	0.5	15	1100	<1	Evaporation of charge
	50	0.5	7.5	1100	~50	Uniform surface
Firing temp.	50	1	15	1150	<1	Evaporation of charge
	50	1	15	1100	~80	Uniform surface
	50	1	15	1050	N/A	Incomplete melting
Flux ratio	50	1	15	1100	~80	Uniform surface
	70	1	15	1100	N/A	Discontinuous film

loading and/or high firing temperatures, the ferrite films were thin or the mixture was subject to excessive evaporation. At a temperature of 1100 °C, where thicker liquid layers were stable, the thickness of the ferrite film could be controlled by varying the surface loading density. Crystalline films of 50–100 μm in thickness were grown. When the firing temperature was reduced to 1050 °C, the mixture did not completely melted and no crystal was formed. However, if the powder was over loaded, even under the same circumstances, the excess melt would run off the substrate, leading to incomplete crystal growth. When the ratio of salt to FOP was 7:3, for example, the evaporation rate was much higher than the 1:1 mixture. Discontinuous films resulted when the maximum temperature was 1100 °C, and crystalline films of ~25 μm resulted when $T_{max} = 1050$ °C.

The mechanism for the growth can be interpreted by Marangoni convection.[16] The system is viewed as a shallow liquid layer heated from below, supported below by a rigid plane and above with a free surface whose surface tension depends linearly upon temperature.[17] A toroid convection pattern develops in which the fluid is observed to rise along the surface of the spherical droplet and to accelerate downwards in the interior towards the liquid/solid contact point. The internal dynamics arise due to the presence of a vertical temperature gradient leading to a gradient in surface tension that in turn drives fluid away from the contact point along the interface. Two time scales associated with two flow scales of the Marangoni and buoyant convection are expected for such a system. The ratio of flow scales is estimated as follows:

$$\frac{U_M}{U_B} \sim \frac{\tau_B}{\tau_M} \sim \frac{\alpha \Delta T}{\Delta \rho g a^2} \sim \frac{\alpha}{\alpha_t \rho g a^2}. \quad (1)$$

Here, convective time scales for flow driven by density gradients and for flow driven by surface tension gradients are τ_B and τ_M, the characteristic velocity of Marangoni flow scales is U_M, and the characteristic velocity associated with buoyancy-driven convection is U_B. In the present case, gravity g is 9.8 m s^{-2}, density ρ is $\sim 5.3 \times 10^3$ kg m^{-3}, change in surface tension due to temperature $\alpha = \partial\sigma/\partial T$ is ~ -0.05 to -0.13×10^{-3} kg s^{-2} K^{-1},[18] the coefficient of thermal expansion is ~17 to 20×10^{-6} K^{-1} (Ref. 19), and characteristic radius a of the droplets is about 5 mm. Therefore, the right side of Eq. (1) can be estimated to be 2.18–5.67, yielding $U_M/U_B > 1$. This indicates that Marangoni flow is the leading current so as to enhance the circulation within the liquid layer and to evaporate the flux. In our case, a low-density salt compared to the heavier density ferrite powder was chosen to accelerate and assist in Marangoni flow. The flux was packed on the bottom of the interface of substrate, when heated, the flux melts and floats upward and leaves the ferrite fluid deposited on the bottom. When the diffusion rate is larger than the evaporation rate a crystal forms.

X-ray diffraction (XRD) spectra as the linear intensity versus $\theta-2\theta$, for the best Zn_2Y films grown using method D at 1100 °C for 15 h with the weight ratio of 1:1 between salt and ferrite powder and surface loading of 1.33 mg/mm^2 were collected at room temperature using Cu Kα radiation in θ-2θ geometry (see Fig. 2(a)). It is noticed that the Zn_2Y film exists as a pure phase structure possessing a strong (00l) preferred crystallographic orientation. Peaks near 37.1° and 78.6° in 2θ correspond to the MgO substrate. Peaks at 24.5°, 30.8°, 43.6°, and 57° correspond to (0012), (0015), (0021), and (0027) planes of the Zn_2Y film, respectively. Lattice constants of the Zn_2Y were obtained by analysis of the XRD data and resulted in a c-axis of 42.94 Å and a-axis of 5.97 Å. The lattice constant a of MgO and the Zn_2Y crystal was measured to be 4.21 and 5.88 Å, respectively. However, the lattice mismatch between the atomic spacing on the (111) plane of the MgO (5.96 Å) and the Zn_2Y crystallographic planes is ~1.34%; this relatively small mismatch is a critical factor in achieving high quality epitaxial growth. To further characterize the crystal quality of the Zn_2Y films, pole figures[20] were collected from the (0015) and (0021) diffraction peaks, and the data are shown as Figs. 2(b) and 2(c), respectively. The reflections in which the angle between the film normal and the vector bisecting the incident and detected x-ray beams, φ, was varied from 0° to 90°, and the azimuthal angle about the bisecting vector, ξ, was varied from 0° to 360°. The sharp peak at the center of the (0015) pole figure indicates c-axis alignment normal to the film plane with low in-plane dispersion. The six-fold symmetry of low intensity peaks arising from {113} Zn_2Y planes has similar values in d spacing. With regard to the (0021) peak reflection, three MgO {200} reflections in which $2\theta = 43.005°$ appear with threefold symmetry. These results confirm the epitaxial growth of Zn_2Y (00l) films on MgO (111) substrates.

The surface morphology of the best Zn_2Y films was observed in scanning electron microscopy (SEM) and presented as Fig. 3(a). Hexagonal crystals, ~1 mm in effective diameter, were clearly visible on the film surface, as shown in Fig. 3(a), qualitatively confirming the orientation of crystals with the crystallographic c-axis aligned normal to the film plane. The thickness of the film was determined by

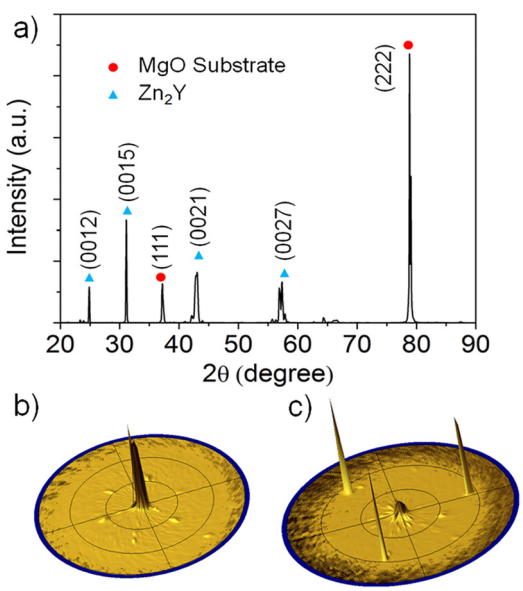

FIG. 2. (a) XRD patterns for Zn_2Y films grown at 1100 °C, (b) pole figure obtained from the (0015) peak reflections, and (c) pole figure obtained from the (0021) peak reflections. During pole figure measurements the angle between the film normal and the vector bisecting the incident and detected x-ray beams, φ, was varied from 0° to 90°, and the azimuthal angle about the bisecting vector, ξ, was varied from 0° to 360°.

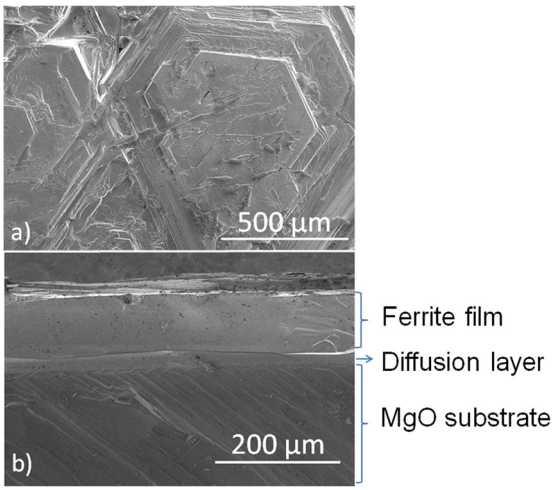

FIG. 3. (a) SEM image of the surface of Zn_2Y thick film, and (b) SEM image of the cross section view of the Zn_2Y film and MgO substrate.

cleaving the MgO substrate and film perpendicular to the plane of the film. The cleavage propagated through both the MgO substrate and the ferrite film so that it was possible to examine both the thickness of ferrite films and the MgO substrate in cross section as shown in Fig. 3(b). The thickness was measured to be $\sim$100 μm. The chemical composition of the Zn_2Y films was determined using energy-dispersive X-ray spectroscopy (EDXS). Findings indicate less than 1% of sodium remained in the Zn_2Y ferrite films, which confirmed that this growth methodology is relatively simple, cost effective, and an environmentally friendly way of depositing thick ferrite films with high purity and crystalline quality.[21,22]

The main ferromagnetic resonance (FMR) linewidth, ΔH, of 62 Oe as the peak-to-peak in the power derivative was measured at a frequency of 9.6 GHz with an external DC magnetic field of 958 Oe applied along the in-plane direction is shown in Fig. 4. The theoretical resonance condition is given by

$$f = \gamma' \sqrt{H(H + H_A + 4\pi M_s)}, \tag{2}$$

where γ' refers to the effective electron gyromagnetic ratio, 2.8×10^6 Hz/Oe. Substituting the saturation magnetization of 2512 kG and driving frequency 9.6 GHz into the above condition, a magnetocrystalline anisotropy field value was calculated to be 8.797 kOe; this is in good agreement with the 8.9 ± 0.1 kOe measured by VSM.

In summary, Zn_2Y ferrite films were grown on MgO (111) substrates by a relatively simple, cost effective, and environmentally friendly crystal growth technique. In order to optimize the growth of films, variation of firing time, temperature, weight ratio of salt to FOP, and ferrite surface loading were explored. Room temperature $\theta-2\theta$ X-ray diffraction measurements indicated all diffraction features correspond to reflections indexed to a single crystalline phase having space group *R-3m* with (00*l*) preferred orientation. Scanning electron microscopy images reveal large hexagonal crystals of $\sim$1 mm in effective diameter and film thicknesses of $\sim$100 μm. The resulting Zn_2Y films had an anisotropy field value of 8.9 ± 0.1 kOe while retaining a relatively high $4\pi M_s$ of 2.5 ± 0.1 kG. The best films have an FMR power derivative peak-to-peak linewidth of 62 Oe at 9.6 GHz. These

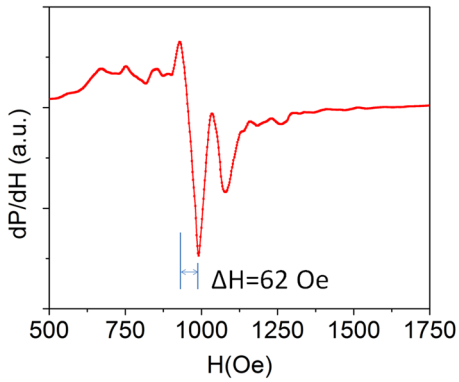

FIG. 4. Ferromagnetic resonance measurement as the peak-to-peak in the power derivative measured at a frequency of 9.6 GHz with an external in film plane field of 0.958 kOe fort he thick Zn_2Y film.

results proved the efficacy of our technique in producing epitaxial growth of thick crystal ferrite films, and lay the foundation for a pathway to realizing thick film based devices that operate at low frequencies (X band to K_u band), and possess the potential to advance microwave device applications.

Professor Richard Gambino of the State University of New York (SUNY) at Stony Brook is gratefully acknowledged for his valuable suggestions during the course of this work. The authors also thank Dr. Zhaohui Chen of the Xtreme Technology Lab, Intel Corporation, Santa Clara, CA for his effort in the early stages of this project.

[1]V. G. Harris, IEEE Trans. Magn. **48**, 1075 (2012).
[2]V. G. Harris, A. Geiler, Y. Chen, S. Yoon, M. Wu, A. Yang, Z. Chen, P. He, P. V. Parimi, X. Zuo, C. E. Patton, M. Abe, O. Acher, and C. Vittoria, J. Magn. Magn. Mater. **321**, 2035 (2009).
[3]V. G. Harris, Z. Chen, Y. Chen, S. Yoon, T. Sakai, A. Gieler, A. Yang, Y. He, K. S. Ziemer, N. X. Sun, and C. Vittoria, J. Appl. Phys. **99**, 08M911 (2006).
[4]B. Hu, Y. Chen, Z. Su, S. Bennett, L. Burns, G. Uddin, K. Ziemer, and V. G. Harris, IEEE Trans. Magn. **49**, 4234 (2013).
[5]Z. Chen, A. Yang, A. Geiler, V. G. Harris, and C. Vittoria, Appl. Phys. Lett. **91**, 182505 (2007).
[6]Y. Chen, M. J. Nedoroscik, A. L. Geiler, C. Vittoria, and V. G. Harris, J. Am. Ceram. Soc. **91**(9), 2952 (2008).
[7]A. Tauber, S. Dixon, and R. O. Savage, J. Appl. Phys. **35**, 1008 (1964).
[8]R. J. Gambino and F. Leonhard, J. Am. Ceram. Soc. **44**, 221 (1961).
[9]H. L. Glass and J. H. W. Liaw, J. Appl. Phys. **49**, 1578 (1978).
[10]Z. Chen, A. Yang, K. Mahalingam, K. L. Averett, J. Gao, G. J. Brown, C. Vittoria, and V. G. Harris, Appl. Phys. Lett. **96**, 242502 (2010).
[11]Y. Chen, T. Sakai, T. Chen, S. D. Yoon, A. L. Geiler, C. Vittoria, and V. G. Harris, Appl. Phys. Lett. **88**, 062516 (2006).
[12]Y. Chen, A. L. Geiler, T. Chen, T. Sakai, C. Vittoria, and V. G. Harris, J. Appl. Phys. **101**, 09M501 (2006).
[13]T. Akashi, K. Matumi, T. Okada, and T. Mizutani, IEEE Trans. Magn. **5**, 285 (1969).
[14]A. Tauber, R. O. Savage, R. J. Gambino, and C. G. Whinfrey, J. Appl. Phys. Suppl. **33**, 1381 (1962).
[15]J. Smit and H. P. J. Wijn, *Ferrrites* (Philips Technical Library, New York/Eindhoven, 1959).
[16]J. Bagard and M. G. Velarde, J. Fluid Mech. **368**, 165 (1998).
[17]D. Tam, V. von Arnim, G. H. McKinley, and A. E. Hosoi, J. Fluid Mech. **624**, 101 (2009).
[18]W. D. Kingery, J. Am. Ceram. Soc. **42**(1), 6 (1959).
[19]R. Krishnan, G. Panneerselvam, M. P. Antony, and K. Nagarajan, J. Nucl. Mater. **403**, 25 (2010).
[20]P. R. Ohodnicki, K. Y. Goh, M. E. McHenry, K. Ziemer, C. Vittoria, and V. G. Harris, J. Appl. Phys. **103**, 07E514 (2008).
[21]B. Hu, Z. Su, S. Bennett, Y. Chen, and V. G. Harris, J. Appl. Phys. **115**, 17A513 (2014).
[22]H. Hibst, Angew. Chem. **4**, 270 (2003).